Desalination and Water Treatment
www.deswater.com
25 (2011) 54–64
January
1944-3994 / 1944-3986 © 2011 Desalination Publications. All rights reserved.
doi: 10.5004/dwt.2011.1416

Removal of textile dyes by sorption on low-cost sorbents. A case study: sorption of reactive dyes onto *Luffa cylindrica*

E.A. Oliveira, S.F. Montanher, M.C. Rollemberg*

Department of Chemistry, State University of Maringá, Av. Colombo, 5790 – CEP 87020-900 Maringá, Paraná, Brazil
Tel. +55 (44) 3261-4332; Fax +55 (44) 3261-4125; email: mcerollemberg@uem.br

Received 15 December 2009; Accepted in revised form 11 July 2010

ABSTRACT

The sorption of reactive dyes Red Procion HE-7B (RP) and Yellow Procion H-4R (YP) on raw *Luffa cylindrica* was examined. Characterization of the sorbent was made by its infrared analysis and also by SEM analysis. The effect of a number of experimental parameters such as sorbent amount, contact time, pH of the dye solution, dye concentration and temperature was evaluated by using the batch technique. The best pH conditions for sorption and desorption are 2.5 and 12. The sorption followed the Langmuir isotherm model, and increasing temperature resulted in increased sorption capacity. Kinetic studies were also carried out and specific rate constants were calculated. Dye sorption experimental data were well fitted to the pseudo second-order kinetic model, and the intraparticle diffusion was also significant. The sorption capacity — 12.2 and 13.9 mg/g for YP and RP, respectively, at 22°C — indicated that this sorbent can be effective for reactive dyes removal. Fixed bed column experiments were also performed and breakthrough curves were obtained. Cycles of sorption/desorption showed a distinct behavior for the dyes; the desorption efficiency of YP increased, achieving 97–98% in the 3rd cycle.

Keywords: Sorption; *Luffa cylindrica*; Reactive dye; Pseudo-second order kinetics; Intraparticle diffusion; Langmuir isotherm model

1. Introduction

Several industries including textile, dyeing and paper industry use dyes to color their products, and it has been estimated that 10–15% of the dyes are lost in the effluent during the dyeing process. Dyes are not always toxic but they have great adverse effects since they are visible pollutants (aesthetic effects) and their presence in water can inhibit aquatic life by reducing light penetration and photosynthesis through the water column [1–3]. Therefore, the color removal from effluents has become environmentally important, and many different treatments have been studied regarding the effectiveness in removing the dyes from effluent and/or decolorizing dyes [4,5]. Several physical, chemical and biological methods have been reported but few have been accepted by textile industries, because the operational costs are usually high [6,7].

Sorption process has been considered a versatile and effective procedure for the removal of dyes and other different pollutants from wastewater. However, although activated carbon is the most widely used sorbent in industry, running costs are still expensive and regeneration for re-use is nearly always difficult [8].

As a consequence, the feasibility of using non-conventional, low-cost materials — such as natural materi-

* Corresponding author.

als, biosorbents, and waste materials from industry and agriculture — for dye removal from effluents has been investigated, and new economical and effective sorbents still need to be exploited [6,9–13].

Reactive dyes are the major group of dyes used in industry; these dyes may contain one or more functional groups capable of forming covalent bonds between the carbon atoms of the dye and the hydroxyl groups in the fiber. Reactive dyes are particularly problematic as they can pass through conventional treatment systems unaffected, and since the chemically active group in the dye molecule can also react with biologically important molecules, reactive dye residues can be greatly harmful to living organisms [14–17].

Luffa cylindrica, a tropical running vine with rounded leaves and yellow flowers, is a sub spontaneous vegetal very common in South America and Brazil. The *Luffa c*. fruit is a 1–2 ft long, cylindrical, smooth skinned gourd and its interior contains white flesh as well as a fibrous structure. This species has found a number of applications, but its main use is still found in the housework. More attractive characteristics of the *Luffa c.* are the physical stability, biodegradability, non-toxicity, availability and low cost. Luffa sorbent is a highly porous and strong biomaterial, made of an open network of fibrous support from the dried fruit of *Luffa c*. The structure of *Luffa c*. is cellulose based and reactive dyes are known to bind covalently with cellulose [17,18]. Therefore, the aim of this work was to study the utilization of *Luffa c.* as sorbent for dye removal from wastewaters by sorption. Effects of parameters such as pH, dye concentration, temperature and sorbent concentration on sorption process were studied. Batch sorption studies were carried out, and kinetic and equilibrium data collected to understand the sorption process.

2. Theory

2.1. Sorption isotherms of dyes

Two sorption isotherm models — Langmuir and Freundlich — were investigated in this work. The Langmuir sorption isotherm, which has been widely applied to describe sorption data, is based on the assumption that maximum sorption corresponds to a saturated monolayer of sorbate molecules on the sorbent surface with constant energy (sorption at homogeneous sites). The linear form of the Langmuir isotherm equation is:

$$C_e / q_r = 1/\left(b Q^{\circ}\right) + C_e / Q^{\circ} \quad (1)$$

q_e (mg/g) and C_e (mg/L) express the equilibrium dye concentration on the sorbent and in the solution, respectively, Q° (mg/g) is the monolayer sorption capacity of the biomass and b (L/mg) is related to the affinity sorbate–sorbent [19,20]. The Langmuir constant K_L (L/g) is related to the partition of the sorbate between the sorbent and the solution, and can be calculated from the relation: $K_L = b\, Q^{\circ}$ [1,21].

The separation factor R_L, a dimensionless constant useful to show the favorability of the sorption process, was calculated from Eq. (2) below, where C_o is the highest initial dye concentration (mg/L). R_L values less than unity reflect a favorable sorption process [22].

$$R_L = 1/\left(1 + bC_o\right) \quad (2)$$

The Freundlich isotherm, the earliest known relationship describing the sorption process, is an empirical equation that describes heterogeneous systems. Eq. (3) shows the linear form of the Freundlich isotherm equation, where K_F (L/g) and n (dimensionless) are the Freundlich sorption constants, indicating the extent and the intensity of the sorption, respectively. The magnitude of the exponent $1/n$ gives an indication of the favorability of the sorption; for a favorable sorption, n must be greater than unity [23,24].

$$\ln q_e = \ln K_F + 1(1/n)\ln C_e \quad (3)$$

2.2. Thermodynamic parameters

From the sorption isotherm data at different temperatures the enthalpy change ($\Delta H^{\circ}_{\text{sorp}}$), entropy change ($\Delta S^{\circ}_{\text{sorp}}$) and free energy change ($\Delta G^{\circ}_{\text{sorp}}$) of sorption could be estimated using Eqs. (4), (5), where K_L is the Langmuir constant (L/mol), T is the solution temperature (K) and R is the universal gas constant (L/mol K).

$$\ln K_L = \Delta S^{o}_{\text{sorp}} / R - \Delta H^{\circ}_{\text{sorp}} / RT \quad (4)$$

$$\Delta G^{\circ} = \Delta H^{\circ} - T\Delta S^{\circ} \quad (5)$$

The plot of $\ln K_L$ vs. $1/T$ yields a straight line from which $\Delta H^{\circ}_{\text{sorp}}$ and $\Delta S^{\circ}_{\text{sorp}}$ can be calculated from the slope and y-intercept, respectively [25,26].

2.3. Sorption kinetics models

Sorption kinetics models can be considered as two main types: reaction-based or diffusion-based models, associated to chemical reactions or mass transfer controlling mechanisms, respectively [27].

The pseudo first-order kinetic model of Lagergren (reaction-based) can be evaluated according to Eq. (6) below, where q_e and q refer to the sorbent dye amount (mg/g) at equilibrium and at any time t (min), respectively, and k_p is the pseudo first-order constant rate (min^{-1}) [28].

$$\ln\left(q_e - q\right) = \ln q_e - k_p / t \quad (6)$$

A pseudo second-order expression based on sorption equilibrium capacity may be written as in Eq. (7), where k_2 is the equilibrium rate constant for pseudo second-order sorption (g/mg min) [28].

$$t/q_t = 1/\left(k_2 q_e^2\right) + t/q_e \quad (7)$$

The constant k_2 has been used to calculate the initial sorption rate, h (mg/g min):

$$h = k_2 q_e^2 \quad (7a)$$

Diffusion-based models consider external and internal diffusion of the sorbate. If the sorbate diffusion within the outside diffusion layer — external diffusion — is the rate-limiting step, the experimental sorption data can be fitted in Eq. (8) successfully.

$$\ln\left(C_t/C_o\right) = -\beta S t \quad (8)$$

$$S = A\,m/V \quad (8a)$$

C_t and C_o are the sorbate concentration in the solution at time t and the initial concentration (mg/L), β is the external diffusion coefficient (m/s) and S is the external surface area of the sorbent (m^2/m^3). S values can be estimated from the interfacial specific surface area (A, m^2/g), the sorbent amount (m, g) and the total sorption volume (V, m^3) according to Eq. (8a). β values can be determined from the slope of the line ln (C_t/C_o) vs. t [29].

Theoretical treatments of intraparticle diffusion involve complex mathematical relations. A simple relation common to most intraparticle diffusion studies is that sorption varies proportionately with one half power of time ($t^{1/2}$). Eq. (9) can be used to describe the sorption kinetic if intraparticle diffusion is the rate-limiting step [30–32].

$$q_t = k t^{1/2} + P \quad (9)$$

From the slope of the line obtained from this equation, the intraparticle diffusion rate parameter k (mg/g $min^{1/2}$) can be determined. According to Weber and Morris [33], when $P \neq 0$ the internal diffusion is not the only rate-limiting step.

An intraparticle diffusion coefficient D (cm^2/s), based on the concentration in solids, was proposed assuming that the sorption rate is independent of the stirring speed and the external mass transfer is non-limiting. The intraparticle diffusion coefficient D can be determined from the slope of the plot of the function log [1 − $(q/q_e)^2$] vs. time [34].

$$-\log\left[1-\left(q_t/q_e\right)^2\right] = \left(4\pi^2/2.3d^2\right)Dt \quad (10)$$

In this equation, d (cm) is the sorbent particle diameter.

3. Materials and methods

For this work, two water-soluble dyes commonly used in the textile industry — Red Procion H-E7B (reactive red 141, RP) and Yellow Procion H-E4R (reactive orange 12, YP) — were selected; the dyes were obtained from a local cotton fabric industry and they were used without any preliminary treatment and/or reaction. YP is a bis(aminochlorotriazine) type dye; its chemical formula is $C_{52}O_{26}N_{18}S_8H_{38}Cl_2$ and the molar weight 1658.46 g/mol. RP is also classified as a bis(aminochlrorotriazine); its chemical formula and molar weight are, respectively, $C_{52}O_{26}N_{13}S_8H_{34}Cl_2$ and 1584.37 g/mol. The dye structures are shown in Fig. 1. Single dye stock solutions were prepared (1000 mg/L) and before the experiments the dye solution was diluted to the desired concentration. All solutions, including the stock solution, were prepared in water purified using a Milli-Q system (Millipore) and analytical grade reagents were used throughout the experiments. The concentration of RP and YP before and after the sorption was determined at 520 nm and 412 nm, respectively, which are the maximum absorption wavelength of the dyes (Hitachi U-2000 Spectrophotometer).

3.1. Preparation and characterization of the sorbent

Mature fruits of *Luffa c*. were collected, dried naturally, washed with distilled water (12 h) and dried in an oven at 70°C for 4 h. The dried material was then ground and sieved to obtain a uniform material. The dried *Luffa c*. sorbent (DL) was characterized by using IR spectrometry (samples of 0.1% in KBr discs, FT-IR Bromem MB–100 spectrophotometer) and the sorbent surface structure was analyzed by scanning electronic microscopy (Shimadzu Superscan SS-550). The BET surface area was determined from N_2 adsorption isotherm with a surface area analyzer (Quantachrome Instruments, Nova 1200).

3.2. Sorption studies

3.2.1. Batch sorption

Sorption experiments were performed at room temperature (22±2°C), unless mentioned, and the batch technique was initially selected due to its simplicity. After pH adjustment (with HCl or NaOH 0.1 mol/L solutions), 20.0 mL of dye solutions, with different initial concentrations, were taken in 50 mL airtight flasks containing a known amount of the dried *Luffa* sorbent. The flasks were agitated mechanically in a water bath maintained at the desired temperature for a pre-determined time. The dye concentrations were measured at time t = 0 and at equilibrium (previously determined) after a filtration step and these values allowed to calculate the amount of dye sorbed (q, mg/g). This procedure was used to evaluate the influence of pH (in the pH range 2–10) and biomass amount (20–400 mg/20.0 mL for 10.0 mg/L dye concentration), and to collect isotherm data. Sorption studies were also performed by batch mode at different temperatures (22°C, 40°C, 60°C). Each experiment was carried out in duplicate, and the mean values are shown; standard relative errors of less than ±4% were found.

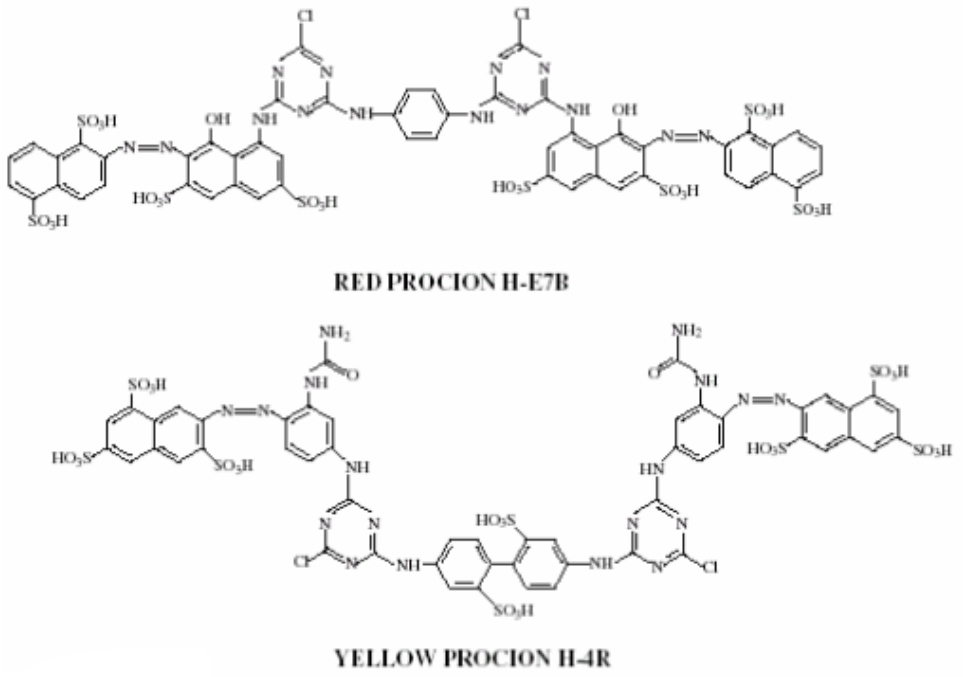

Fig. 1. Chemical structures of reactive dyes Red Procion H-E7B and Yellow Procion H-4R.

3.2.2. Column sorption

Sorption studies with columns were carried out in glass columns of 8 mm of inner diameter and 30 cm of total length. Fixed bed columns were prepared with ca. 1 g of the dry *Luffa* sorbent supported by glass wool (sorbent bed height = 7.2 cm). The optimized flow rate was 4 mL min^{-1}.

The column was loaded with a dye solution (10 mg L^{-1}), at the optimized flow rate, and the column was operated until the effluent concentration matches with the initial dye concentration.

After the sorption the column was percolated with 1000 mL of water or NaOH pH 11, in order to free the dyes. Different aliquots (100 mL) were collected and dye concentration was determined spectrophotometrically. Finally, in order to evaluate the reutilization of the columns, they were loaded with 250 mL of a dye solution (10 mg L^{-1}). The sorbed dyes were then eluted with 200 mL aliquots of NaOH pH 11 and the columns were regenerated with deionized water. This procedure was repeated four times.

4. Results and discussion

4.1. Sorbent characterization

Like all vegetable biomass, *Luffa c*. is composed of cellulose, hemi-cellulose and lignin. FT-IR spectrum allowed the identification of some of the functional groups which are probably involved in the sorption process (Fig. 2). The broad band found in the region of 3400 cm^{-1} indicated the presence of OH groups on the dried Luffa surface. The signal at 2930 cm^{-1} could be assigned to C–H stretching [20]. The band at 1645 cm^{-1} was associated to carbonyl groups of amides. In the region of shorter wave number, the peaks were attributed to vibrations involving C–O–C and OH of polyssacarides and C–O of alcohols (1110–1020 cm–1). Therefore, the IR-spectrum of the DL indicated the existence of groups that are strongly affected by the pH of the solutions, and which are able to interact with dye molecules.

The specific surface area *S* (BET method) of DL particles was 6.2 m^2/g, and the *Luffa* particle sizes were in the range of 75–425 μm, with an average diameter of 300 μm. This average diameter was calculated by using a simple sieving procedure, with a set of sieves of different openings; the average diameter value was estimated from the average of the different fractions, considering the total mass of sorbent used in the experiment.

The surface structure of DL sorbent was examined in a scanning electron microscope (Fig. 3), which has been a key tool for characterizing the surface morphology and fundamental physical properties of the sorbent. The SEM also reveals an irregular, fragmented surface, and a structure with layers, which suggests an adequate morphological structure to sorption processes. From Fig. 3, DL has a fiber structure with a number of fissures and macropores where is possible for dyes to be trapped and sorbed.

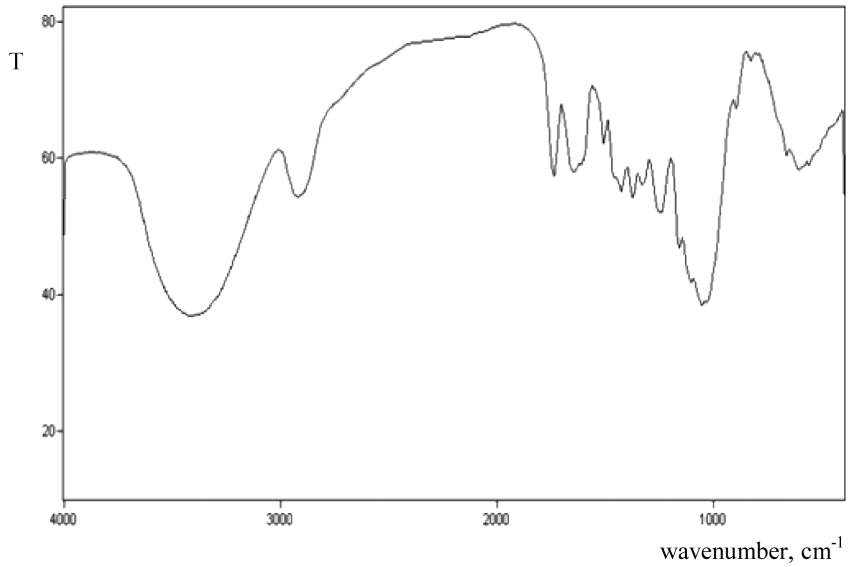

Fig. 2. FTIR spectrum of DL sorbent.

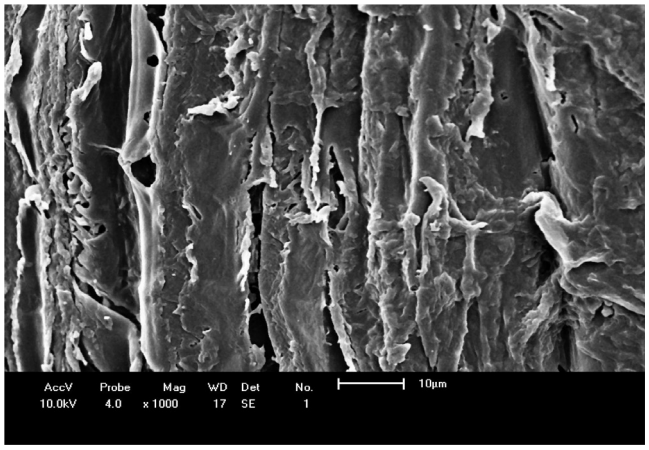

Fig. 3. SEM of raw *Luffa cylindrica* (particle size ≤425 μm). Magnification: ×1000.

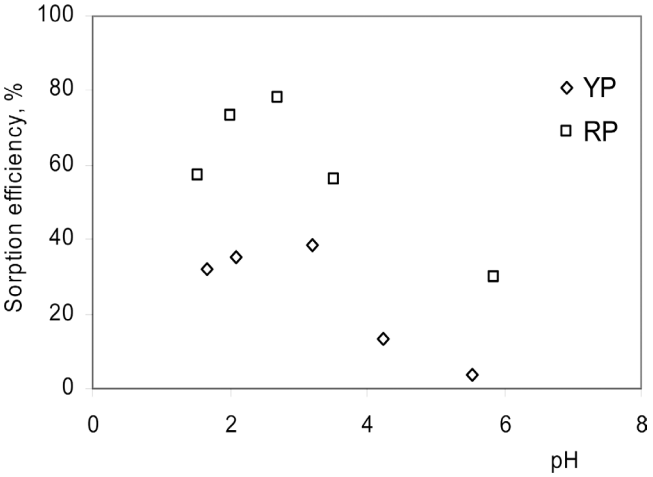

Fig. 4. pH effect on the sorption of Red Procion and Yellow Procion onto DL sorbent. Experimental conditions: initial dye concentration 10 mg/L; DL amount 100 mg; total volume 20 mL; contact time 60 min; temperature 22°C.

4.2. Sorption conditions

YP and RP dye present ionizable groups in their structures. For these dyes, the sorption efficiency was greater at low pH; the RP and YP sorption on dried *Luffa* sorbent increased gradually with decreasing solution pH up to pH 4 and then a sharp increase was observed between pH 4 and 2.5 (Fig. 4). Maximum dye removal was found at pH 2.5. This behavior can be explained considering the biomass surface charge due to ionizable groups, which can lose or accept protons according the solution pH. At low pH values the biomass surface groups are protonated and the surface is positively charged; at higher pH values, the surface groups loose protons and the surface becomes negative. Maximum YP and RP sorption efficiency were found at pH ca. 2.5, where sulphonic groups in the dye molecules are dissociated ($R\text{-}SO_3^-$). There is probably a strong electrostatic attraction between the positive biomass surface (due to the protonation of the functional groups) and the negatively charged dye molecules. At pH above 5–6, at which the carboxylic groups on the surface of DL are considered to be highly deprotonated (negative surface charge), the dye sorption was very poor. The YP sorption was lower than that of RP, but at a fixed pH (e.g., 2.5) the surface charge density of the Luffa sorbent is constant and independent of the sorbate and, as a consequence, the coulombic attraction of the positive charge on the sorbent surface is the same for both dyes. Therefore, the dye chemical structure characteristics — shape,

number of active groups, stability of a negative charge, and others — must give the difference in the affinity of the dyes toward the sorbent.

With an increase in the sorbent concentration, from 1.0 to 20 g/L, YP and RP removal increased from 20 to 60% and from 60 to 90% respectively, as the number of possible sorbing sites becomes greater. However, the dye removal per unit weight of *Luffa* biosorbent (q, mg/g) decreased for both the dyes studied, suggesting that a more economical removal can be carried out using small batches of sorbent rather than in a single batch. So, 1.0 and 2.5 g/L were chosen as the optimal sorbent concentrations for RP and YP removal, respectively.

Both these experiments were carried out fixing a contact time of 60 min, according to the preliminary kinetic studies (see Fig. 7).

4.3. Sorption isotherms

In order to understand the mechanisms of dye sorption and also to evaluate the temperature effect on sorption process, the sorption isotherms for the two dye–DL systems were obtained. The experiments were carried out under the optimum condition that includes initial pH about 2.5 and 60 min of contact time. At concentrations in the range of 5–100 mg/L (Figs. 5, 6) the sorption process can be seen with three different stages. First, there is fast sorption as a result of the rapid attachment of YP and RP to the *Luffa* sorbent surface. In the second stage, the sorption is slower, probably because it takes place in the pores of the solid and finally, in the third and last stage, the sorption attains the equilibrium.

The experimental data were studied following the two isotherm equations of Langmuir and Freundlich [Eqs. (1) and (3)]. The parameters calculated according to these models, which are given in Table 1, show that dye sorption structure and temperature affect the sorption process. The data in Table 1 clearly indicate that YP and RP sorption capacities increase with increasing temperature. The temperature has two major effects on the sorption process. First, increasing temperature is known to increase the rate of diffusion of sorbate molecules across the external boundary layer and in the internal pores of the sorbent particle, due to the decrease in the viscosity of the solution. In addition, changing the temperature will change the equilibrium capacity of the sorbent for a particular sorbate [35].

The mechanism of RP and YP sorption on *Luffa* sorbent cannot be concluded directly from the Freundlich or Langmuir fitting. However, from Table 1 it can be concluded that the sorption data over a concentration range 5–100 mg/L are well represented by the Langmuir

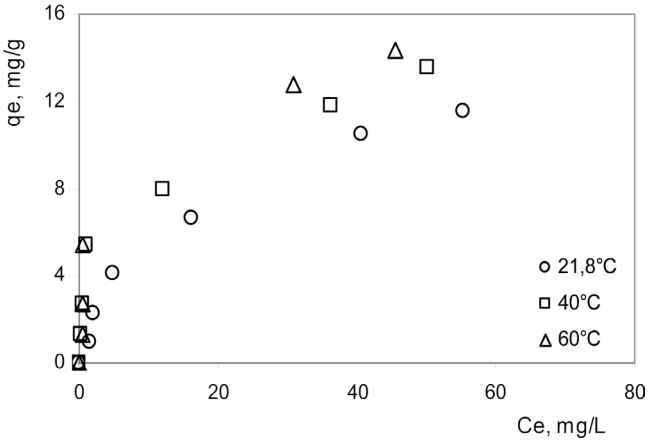

Fig. 6. Sorption isotherms for Red Procion on DL sorbent at different temperatures according to the Langmuir model. Experimental conditions: DL concentration 1.0 g/L; pH 2.5; contact time 60 min.

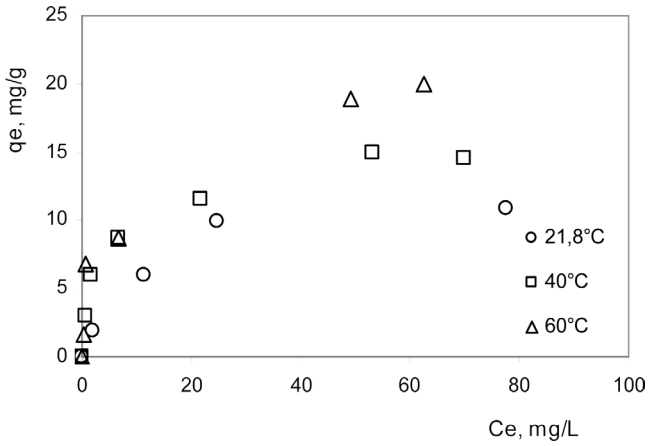

Fig. 5. Sorption isotherms for Yellow Procion on DL sorbent at different temperatures according to the Langmuir model. Experimental conditions: DL concentration 2.5 g/L; pH 2.5; contact time 60 min.

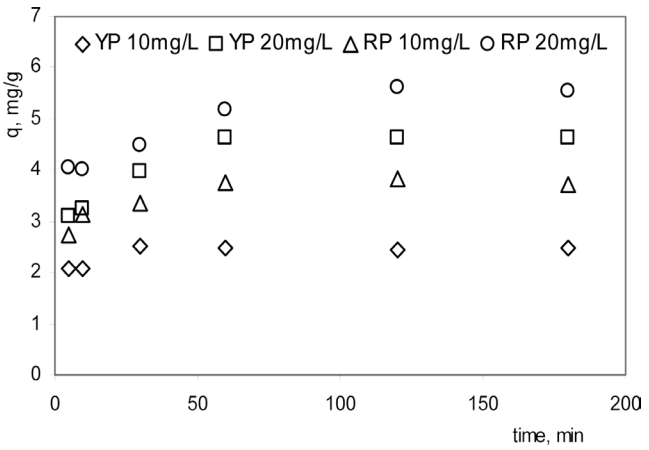

Fig. 7. Time effect on the sorption of Yellow Procion and Red Procion on DL sorbent. Experimental conditions: DL concentration (YP) 2.5 g/L; DL concentration (RP) 1.0 g/L; pH 2.5; contact time 60 min; temperature 22°C.

Table 1
Sorption isotherm constants for the sorption of Red Procion (RP) and Yellow Procion (YP) on DL sorbent

	Freundlich				Langmuir			
	T (°C)	K_F (L/g)	n	r^2	Q_{max} (mg/g)	b (L/mg)	r^2	R_L
YP	22	1.57	2.01	0.9113	12.2	0.117	0.9848	0.086
	40	4.12	2.99	0.9333	15.5	0.233	0.9885	0.045
	60	6.97	4.16	0.8501	18.7	0.275	0.9725	0.039
RP	22	1.76	2.09	0.9703	13.9	0.0784	0.9303	0.12
	40	3.86	3.19	0.9598	13.8	0.268	0.9783	0.039
	60	6.30	4.61	0.9870	15.1	0.367	0.9876	0.029

isotherm model ($r^2 > 0.93$), suggesting a monolayer sorption (but not necessarily a compact monolayer) and also suggesting that DL sorbent surface is mostly made up of homogeneous sorption sites. The Langmuir parameter Q^o indicates the maximum sorption capacity of dried Luffa sorbent, that is, the dye sorption at high concentrations — a case closer to the characteristics of industrial effluents. The values in Table 1 indicate a similar behavior profile for both YP and RP sorption since Langmuir parameters values are very comparable. However, it seems that the temperature has a more significant effect on sorption for YP while a less influence for RP.

Langmuir separation factor R_L values [Eq. (2)], also shown in Table 1, lie between 0 and 1, confirming thereby the favorable sorption process; so, dried *Luffa* sorbent exhibits a good potential for dye removal from water.

The sorption of YP at higher temperatures is greater than that of RP and this may be due to the different molecular shapes and sizes. In general, the biggest molecule offers greater resistance to penetration into the sorbent pore structure. However, when large molecules presenting dipoles and polar groups are sorbed the dispersion force energy can be greater than the electrostatic interaction energy. As a result, the sorbed molecule presents a forced dipolar orientation with respect to the surface electrostatic field, and this can affect the sorption [26].

The Freundlich parameters in Table 1 show a favorable sorption ($n > 1$) at all cases, with similar sorption (K_F) for both dyes. Increasing temperature increased the Freundlich constants, that is, increased both sorption favorability and extension. McKay et al. [20], reporting on the sorption of dyes on chitin, observed that an increase in temperature resulted in increasing sorption capacity – as it was found in this work for RP and YP sorption on *Luffa* sorbent. The increased sorption capacity with increasing temperature can be related to an increase in the amount of sorption sites in the sorbent surface, which was originated as a result of some breaking of internal bonds in the proximity of the surface. Another aspect is a consequence of the sorbent porosity, because increasing temperatures can favor the dye diffusion within the pores of the sorbent.

4.4. Thermodynamic parameters

The thermodynamic parameters (Table 2) were determined according to Eqs. (4), (5). The negative values of ΔG^o_{sorp} indicate the viability and spontaneous nature of RP and YP sorption on Luffa sorbent. The free energy change values obtained for YP–DL and RP–DL systems decrease with increasing temperature, which in turn increase the sorption capacity (Table 1). In general, the change of free energy for physiosorption is between –20 and 0 kJ/mol, and for chemisorption the values lie between –80 and –400 kJ/mol [3]. In this study, ΔG^o_{sorp} values for the dye sorption process were approximately –25 kJ/mol, suggesting that the interaction between the sorbent and dye molecules is not only physical, and that there is also some kind of chemical interaction. Such interactions involve electrostatic attraction, covalent bonding, non polar interaction, water binding and/or hydrogen-type bonding between the dye molecules and the sorbent structure and between sorbed dye molecules [26].

Electrostatic interaction forces between dye molecules and *Luffa* sorbent structure are certainly involved because the dyes molecules have a negative charge and the sorbent has a positively charged surface at acidic pH. In addition to electrostatic interactions, there is the possibility of H-bond and/or water bridge formation between groups in the sorbent structure (such as amine and carboxylate) and OH groups present in the dye structure. The existence of

Table 2
Thermodynamic parameters for the sorption of Red Procion (RP) and Yellow Procion (YP) on DL sorbent

	T (°C)	$\Delta G°$ (kJ/mol)	$\Delta H°$ (kJ/mol)	$\Delta S°$ (J/mol K)
YP	22	–19	28	159
	40	–22		
	60	–25		
RP	22	–18	38	190
	40	–22		
	60	–25		

H-bonds and water bridges between the sorbent and the dyes helps to increase the total interaction energy, leading to a higher enthalpy of sorption.

The RP and YP sorption process is endothermic ($\Delta H^{o}_{sorp} > 0$), and this confirms the increasing of the sorption capacity with increasing temperature. The positive and relatively high values of the enthalpy change (28 and 38 kJ/mol) also indicate that the dye sorption is not only physical in nature. According to Messina and Schulz the existence of H-bonds and water bridges between the sorbent and the sorbate increases the total interaction energy, leading to a high enthalpy of sorption [26]. The positive entropy change values correspond to an increased randomness at the solid/solution interface and reflect good affinity of the dye toward the dried *Luffa* sorbent [35].

4.5. Sorption kinetics

Kinetic studies were carried out for two different RP and YP concentrations. The effect of contact time on the dye sorption on *Luffa* sorbent is shown in Fig. 7. When the contact time is increased, the sorption capacity is also increased, and a maximum is observed at 60 min, beyond which there was almost no further increase in the sorption capacity. Thus, 60 min was fixed as the equilibrium contact time.

Kinetic data were evaluated with the pseudo first-order kinetic model. The relationship in Eq. (6) was not linear over the entire time range ($r^2 < 0.89$), indicating that the experimental data did not agree well with this model [28,30].

However, experimental data of RP and YP sorption on dried *Luffa* sorbent obey the pseudo second-order kinetic model. Values of k_2 and q_e that were calculated from Eq. (7) are shown in Table 3. The correlation coefficients for the pseudo second-order kinetic plots are greater than 0.994 and the calculated equilibrium sorption capacities q_e agree with the experimental q_e values; therefore, there is strong positive evidence that the dye sorption on this sorbent follows the pseudo second-order kinetic expression. This has already been observed for the sorption of a number of dyes on different solid sorbents [36]. The change of the pseudo second-order rate constants with dye concentration is also given in Table 3. The k_2 values decrease with the increase of RP and YP initial concentration.

It is well known that sorption kinetics shows large dependence on the physical and chemical characteristics of the biosorbent, which also influence the sorption mechanism. The solute transfer process is assumed to proceed through a succession of steps. In short, the solute is firstly transferred from the bulk solution to the boundary film, transported from the boundary film to the surface of the sorbent (external diffusion), and then transferred from the surface of the sorbent to the intraparticle active sites (intraparticle diffusion); finally, the solute species are retained on the active sites in the sorbent. The first step is thought non limiting as the stirring is sufficient to avoid a concentration gradient in the solution. Therefore, external and intraparticle diffusion resistance are significant controlling steps [37].

The kinetic parameters, determined according to Eqs. (6)–(10), are shown in Table 4. According to Weber and Morris model [Eq. (9)], the plot of q_t vs. $t^{1/2}$ has to be linear if intraparticle diffusion is involved in the sorption process; besides, when the line pass through the origin, the intraparticle diffusion is the rate-limiting step [32]. If the line does not pass through the origin the intraparticle diffusion is not the only rate-controlling step, and other kinetic mechanisms, which operate simultaneously, may limit the sorption rate. This relationship for the RP and YP sorption on dried Luffa sorbent is not linear for the entire range of reaction time, and the straight line does not pass through the origin (figures not shown). This has been also found in the sorption of other dyes by lignocellulosic wastes [38]. This non-linearity has been explained in terms of different diffusion processes having an effect on the sorption [39]. As shown in Table 4, increasing the initial dye concentration promotes the diffusion in the DL sorbent, resulting in an increase in the intraparticle diffusion rate.

If dye sorption occurs on the external surface of the sorbent, Eq. (8) should describe the sorption data. The YP and RP sorption data on dried *Luffa* sorbent show only a reasonable correlation with external diffusion model, with correlation coefficients $0.71 < r^2 < 0.93$. This would indicate that the sorption of YP and RP probably involves a surface process on the external surface of the sorbent particle. As shown in Table 4, β values decrease when the concentration increases; this behavior can be related to a

Table 3
Pseudo second-order kinetic parameters for dye-DL sorbent systems

	C_0 (mg/L)	q_e (1) (mg/g)	q_e (2) (mg/g)	k_2 (g/mg min)	h (mg/g min)	r^2
YP	10.0	2.47	2.48	0.49	3.03	0.9997
	20.0	4.64	4.80	0.052	1.20	0.9990
RP	10.0	3.78	3.80	0.14	1.97	0.9946
	20.0	5.94	5.94	0.027	0.96	0.9973

(1) experimental value (2) value from Eq. (7)

Table 4
Kinetic parameters for the dye–DL sorbent systems

	C_0 (mg/L)	External diffusion		Intraparticle diffusion			
		β (m/s)	r^2	D_i (cm²/s)	r^2	k_d (mg/g s$^{1/2}$)	r^2
YP	10.0	8.5×10^{-8}	0.7196	9.4×10^{-9}	0.9480	4.9×10^{-3}	0.9737
	20.0	6.0×10^{-8}	0.8983	3.3×10^{-8}	0.9556	1.7×10^{-2}	0.9496
RP	10.0	4.3×10^{-7}	0.9246	2.7×10^{-9}	0.9932	1.1×10^{-2}	0.9464
	20.0	2.9×10^{-7}	0.9205	7.5×10^{-9}	0.9882	2.3×10^{-2}	0.9643

higher competition for the sorption surface sites at higher sorbate concentrations, thus lowering the sorption rate.

The internal diffusion seems to be of major importance in the YP and RP sorption on dried *Luffa* sorbent. The internal diffusion models which had been evaluated in this work show a very good fit for YP and RP sorption experimental data, with correlation coefficients higher than 0.94 (Table 4). Intraparticle diffusion is involved in the sorption process above five minutes and prior to this the process seems to be controlled by an external diffusion mechanism. From Table 4 it is observed that the changes in β values due to dye concentrations are much smaller than those in D and k_d values. This behavior also suggests that internal diffusion is the controlling mechanism during dye sorption. However, D values (≈10^{-8}–10^{-9}) indicate that intraparticle diffusion is not the only rate controlling step, and both boundary layer (external diffusion) and intraparticle diffusion might be involved in the dyes sorption on *Luffa* sorbent.

All these observations allow supposing that the sorption of RP and YP takes place probably via surface reactions until the functional sites are fully occupied; then, dye molecules diffuse into the pores of the *Luffa* sorbent for further reaction. Similar results have been reported for a number of ligninic sorbents, which presents functional groups that are able to be involved in the reactions with dye ions [30].

Desorption studies can also help to elucidate the sorption mechanisms. Therefore, RP and YP desorption studies were carried out, and neutral pH water, acidic and alkaline solutions were selected as desorbing agents. HCl solution (0.1 mol/L) and water were not able to recover significant amounts of the sorbed dyes (desorption efficiency <5%), and this indicates that the sorption is not only due to weak bonds. However, a NaOH solution with pH = 12 recovered ca. 50% of RP and YP dyes. Therefore, the sorption mechanism involved electrostatic interactions between the dyes (negatively charged) and the sorbent surface, which is protonated and negatively charged at low and higher pH values, respectively [30].

4.6. Column sorption experiments

Fixed bed columns are highly efficient in sorption/desorption cycles, as usually found in the industries, because the concentration gradient acts as an important 'driving force' for the sorption process. Therefore, a number of fixed bed columns experiments were performed in order to compare batch and columns systems for the dye removal with Luffa c. sorbent.

Breakthrough curves for RP and YP dyes sorption in Fig. 8 show an effluent concentration nearly zero (C/C_o < 0.01) at 60 mL (RP) or 40 mL (YP), increasing after this volume (breakthrough point). Column exhaustion (C/C_o > 0.9) was observed at 320 mL (YP) and 400 mL (RP). The exhaustive capacity can be estimated from the area below the breakthrough curve [40,41], according to Eq. (11):

$$Q\left(\text{mg g}^{-1}\right) = \text{(area above the curve)} \times C_o\left(\text{mg L}^{-1}\right) / \text{sorbent amount (g)} \quad (11)$$

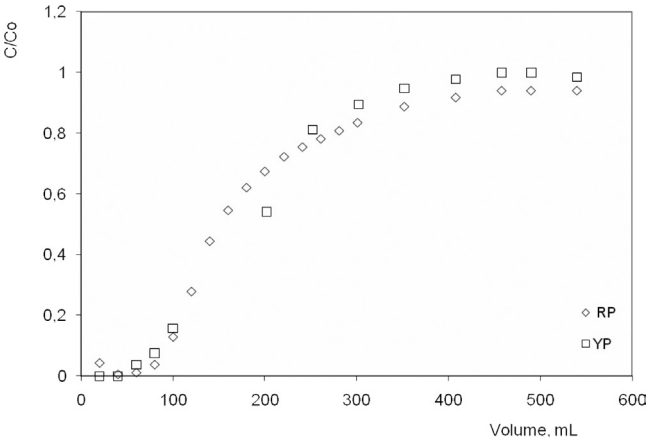

Fig. 8. Breakthrough curves for the sorption of Yellow Procion and Red Procion. Experimental conditions: C_o 10 mg L^{-1}; pH 2,8; m (sorbent) 1.174 g; fixed bed height 7.2 cm; flow rate 4 mL min^{-1}.

The sorption column capacities for RP and YP, calculated according to this expression, are 4.0 mg g^{-1} and 3.2 mg g^{-1}, respectively. These values are small if compared to the Langmuir values (Table 1), but some authors have mentioned that the sorption parameters obtained with fixed bed column and batch systems do not agree, due to the presence of different mechanisms [42]. Sorption efficiency was 92% and 89% for RP and YP dye, respectively.

For most of industrial applications, the disposal of sorbents as waste is not an economic option and therefore regeneration is carried out to an extent that the sorbents can be reused. So, *Luffa* sorbent regeneration was investigated. Water (pH = 7) and alkaline solutions were tested as desorbing agents. Water was not able to remove the dyes efficiently, and this suggests that the sorption involves not only weak bonding. However, NaOH pH 11 removed significant amounts of the sorbed dyes from the column. Increasing the pH results in an increasing number of negative sites at the sorbent surface, and this favors the dyes desorption due to the electrostatic repulsion. The YP and RP desorption were 92% (150 mL) and 94% (300 mL), respectively, according to the curves in Fig. 9.

In this study, four consecutive cycles of sorption / desorption were performed, using a NaOH solution (pH = 11) as a desorbing agent, and dyes recuperation was distinct (Table 5). The desorption efficiency for RP dye remained unaltered in the four cycles, around 75%; but desorption efficiency for YP dye increased, achieving 97–98% in the two last cycles (Table 5). So, it seems that NaOH is very efficient in the recuperation of YP, but less efficient in the RP recuperation.

Table 5 also shows the sorption efficiency in the four successive cycles. No significant variation was found for RP. However, the sorption of YP dye decreased from the first to the fourth cycle. This fact could be attributed to non-expected residual amounts of NaOH (that is, increased pH) during the experiments with the yellow dye, even considering the washing step with deionized water before a new cycle.

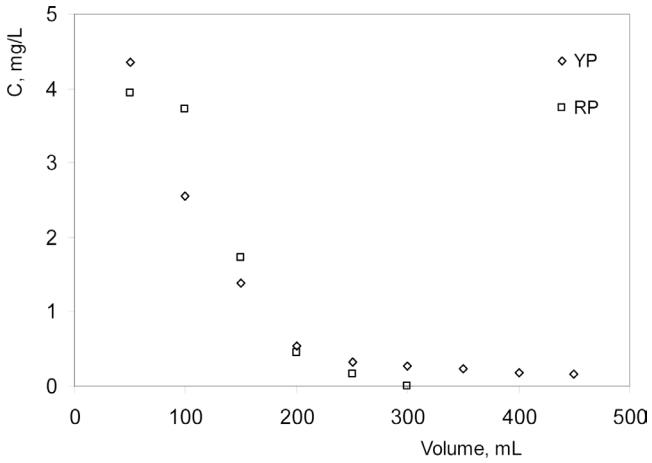

Fig. 9. Desorption curves for Yellow Procion and Red Procion dyes. Experimental conditions: *C* (eluent) 0.001 mol NaOH L^{-1}; *m* (sorbent) 1.174 g; fixed bed height 7.2 cm; flow rate 4 mL min^{-1}.

Table 5
Desorption (E_{des}) and sorption (E_{sor}) efficiency in successive cycles for Red Procion (RP) and Yellow Procion (YP)

Cycle	YP		RP	
	E_{des}, %	E_{sor}, %	E_{des}, %	E_{sor}, %
1	83		77	
2	74	100	78	98
3	98	76	72	99
4	97	75	80	96

The desorption behavior of NaOH indicated that it is not a completely efficient desorbing agent. However, is very expressive the sorption efficiency for RP dye in all the cycles, and is also very satisfactory (> 72%) the dyes recuperation.

5. Conclusion

The present work evaluated the potential of raw *Luffa c*. in sorption processes. The study showed that the dried *Luffa* sorbent can be an attractive alternative for the removal of Red Procion and Yellow Procion dyes from aqueous solution. The sorption follows the Langmuir isotherm model, while the kinetic data are well fitted by the pseudo second-order kinetic model, and the fitting by intraparticle diffusion model is only slightly worse. Probably the sorption in the initial stage is due to boundary layer diffusion, whereas the later stage is due to the intraparticle diffusion. Thermodynamic parameters obtained for both dyes indicate that the sorption process is spontaneous and endothermic in nature. Fixed bed column experiments allowed revealing the high sorption efficiency for RP dye and also, a very satisfactory ability (> 72%) to recuperate the dyes from the column. The overall dye recuperation efficiency, determined after four cycles of sorption/desorption, was 77% and 86% for RP and YP, respectively. These values are very attractive looking for economical processes. Although the *Luffa* sorbent does not have a high sorption capacity if compared with other sorbent, especially with sorbent such as activated carbons, it is a very attractive material due to its low-cost, availability and biodegradability.

References

[1] M.A. Al-Ghouti, M.A.M. Khraisheh, S.J. Allen and M.N. Ahmad, The removal of dyes from textile wastewater: a study of the physical characteristics and adsorption mechanisms of diatomaceous earth. J. Environ. Manage., 69 (2003) 229–238.

[2] V.K.Garg, R. Gupta, A.B. Yadav and R. Kumar, Dye removal from aqueous solution by adsorption on treated sawdust, Bioresour. Technol., 89 (2003) 121–124.
[3] S. Tunali, A.S. Özcan, A. Özcan and T. Gedikbey, Kinetics and equilibrium studies for the adsorption of Acid Red 57 from aqueous solutions onto calcinde-alumnite, J. Hazard. Mater., 135 (2006) 141–148.
[4] P. Nigam, G. Armour, I. Banat, D. Singh and R. Marchant, Physical removal of textile dyes from effluents and solid-state fermentation of dye-adsorbed agricultural residues, Bioresour. Technol., 72 (2000) 219–226.
[5] T. Robinson, B. Chandran and P. Nigam, Removal of dyes from a synthetic textile dye effluent by biosorption on apple pomace and wheat straw, Wat. Res., 36 (2002) 2824–2830.
[6] S.M. Ghoreishi and R. Haghighi, Chemical catalytic reaction and biological oxidation for treatment of non-biodegradable textile effluent, Chem. Eng. J., 95 (2003) 163–169.
[7] M. Rachakornkij, S. Ruangchuay and S.S. Teachakulwiroj, Removal of reactive dyes from aqueous solution using bagasse fly ash, J. Sci. Technol., 26 (2004) 13–24.
[8] G.M. Walker, L. Hansen, J.A. Hanna and S.J. Allen, Kinetics of a reactive dye adsorption onto dolomitic sorbents, Wat. Res., 37 (2003) 2081–2089.
[9] G. Crini, Non-conventional low-cost adsorbents for dye removal: A review, Bioresour. Technol., 97 (2005) 1061–1085.
[10] T. Robinson, G. McMullan, R. Marchant and P. Nigam, Remediation of dyes in textile effluent: a critical review on current treatment technologies with a proposed alternative, Bioresour. Technol., 77 (2001) 247–255.
[11] A.E. Ofajama, Equilibrium sorption of mehtylene blue using mansonia wood sawdust as biosorbent, Desal. Wat. Treat., 3 (2009) 1–10.
[12] M.M. El-Latif and A.M. Ibrahim, Adsorption, kinetic and equilibrium studies on removal of basic dye from aqueous solutions using hydrolyzed oak sawdust, Desal. Wat. Treat., 6 (2009) 252–268.
[13] N. Bouchemal and F. Addoun, Adsorption of dyes from aqueous solution onto activated carbons prepared from date pits: The effect of adsorbents pore size distribution, Desal. Wat. Treat., 7 (2009) 242–250.
[14] M.A.M. Kharaisheh, Y.S. Al-Degs, S.T. Allen and M.N. Ahmad, Elucidation of controlling steps of reactive dye adsorption on activated carbon, Ind. Eng. Chem. Res., 41 (2002) 1651–1657.
[15] E.J. Weber and V.C. Stickney, Hydrolysis kinetics of reactive blue 19-vinyl sulfone, Wat. Res., 27 (1993) 63–67.
[16] Z.Y. Xu, Q.X. Zhang and H.H.P. Fang, Applications of porous resin sorbents in industrial wastewater treatment and resource recovery, Crit. Rev. Environ. Sci. Technol., 33 (2003) 363–389.
[17] H.S. Ho, C.T. Huang and H.W. Huang, Equilibrium sorption isotherm for metal ions on tree fern, Proc. Biochem., 37 (2002) 1421–1430.
[18] Y.K. Liu, M. Seki, H. Tanaka and S. Furusaki, Characteristics of loofa (*Luffa cylindrica*) sponge as a carrier for plant cell Immobilization, J. Ferm. Bioeng., 85 (1998) 416–421.
[19] I. Langmuir, The adsorption of gases on plane surfaces of glass, mica and platinum, J. Amer. Chem. Soc., 40 (1918) 1361–1403.
[20] G. McKay, H.S. Blair and J.R. Gardner, Adsorption of dyes on chitin. I. Equilibrium studies, J. Appl. Polym. Sci., 27 (1982) 3043–3057.
[21] R.F. Moreira, J.L. Soares, H.J. José and A.E. Rodrigues, The removal of reactive dyes using high-ash char, Braz. J. Chem. Eng., 18 (2001) 327–336.
[22] K.R. Hall, L.C. Eagleton, A. Acrivos and T. Vermeulen, Pore- and solid-diffusion kinetics in fixed-bed adsorption under constant-pattern conditions, Ind. Eng. Chem. Fundam., 5 (1966) 212–223.
[23] H.M.F. Freundlich, Über die Adsorption in Lösungen, Z. Phys. Chem., 57 (1906) 385–470.
[24] W. Fritz and E.E. Schlunder, Isothermal effectiveness factor—II : Analytical expression for single reaction with arbitrary kinetics, geometry and activity distribution, Chem. Eng. Sci., 36 (1981) 721–730.
[25] M.S. Chiou and H.Y. Li, Adsorption behavior of reactive dye in aqueous solution on chemical cross-linked chitosan beads, Chemosphere, 50 (2003) 1095–1105.
[26] P.V. Messina and P.C. Schulz, Adsorption of reactive dyes on titânia-silica mesoporous materials, J. Colloid. Interf. Sci., 299 (2006) 305–320.
[27] H.S. Ho, J.C. Ng and G. McKay, Kinetics of pollutant sorption by biosorbents: Review, Separ. Purif. Methods, 29 (2000) 189–232.
[28] H.S. Ho and G. McKay, The kinetics of sorption of divalent metal ions onto sphagnum moss peat, Wat. Res., 34 (2000) 735–742.
[29] C.K. Lee, K.S. Low and S.L. Chew, Removal of anionic dyes by water hyacinth roots, Adv. Environ. Res., 3 (1999) 343–351.
[30] Y.S. Ho and G. McKay, Pseudo-second order model for sorption processes, Proc. Biochem., 34 (1999) 451–465.
[31] L. Krim, S. Nacer and G. Bilango, Kinetics of chromium sorption on biomass fungi from aqueous solution, Am. J. Environ. Sci., 2 (2006) 27–32.
[32] C.F. Wu, L.R. Tsseng and S.R. Juang, Kinetic modeling of liquid-phase adsorption of reactive dyes and metal ions on chitosan, Wat. Res., 35 (2001) 613–618.
[33] S.A. Brady and J.R. Dungan, Biosorptton of heavy metal cations by non-viable yeast biomass, Environ. Technol., 15 (1994) 429–438.
[34] K. Urano and H. Tachikawa, Process development for removal and recovery of phosphorus from wastewater by a new adsorbent. 2. Adsorption rates and breakthrough curves., Ind. Eng. Chem. Res., 30 (1991) 1897–1899.
[35] S. Wang, Y. Boyjoo, A. Choueib and Z.H. Zhu, Removal of dyes from aqueous solution using flu ash and red mud, Wat. Res., 39 (2005) 129–138.
[36] M. Arami, N.Y. Limaee, N.M. Mahmoodi and N.S. Tabrizi, Equilibrium and kinetics studies for the adsorption of direct and acid dyes from aqueous solution by soy meal hull, J. Hazard. Mater., 135 (2006) 171–179.
[37] S.F. Montanher, E.A. Oliveira and M.C. Rollemberg, Utilization of agro-residues in the metal ions removal from aqueous solutions, In A. Lewinsky, ed., Hazardous Materials and Wastewater, Nova Science Publishers, New York, 2006, pp. 58–85.
[38] K.K. Singh, R. Rastogi and S.H. Hasan, Removal of cadmium from wastewater using agricultural waste 'rice polish', J. Hazard. Mater., 121 (2005) 51–58.
[39] G.S. Gupta, G. Prasad and V.N. Singh, Removal of chrome dye from aqueous solutions by mixed adsorbents: fly ash and coal, Wat. Res., 24 (1990) 45–50.
[40] V.K. Gupta, A. Mittal and V. Gajbe, Adsorption and desorption studies of a water soluble dye, Quinoline Yellow, using waste materials. J. Colloid Interf. Sci., 284 (2005) 89–98.
[41] K. Vijayaraghavan, K. Palanivelu and M. Velan, Crab shell-based biosorption technology for the treatment of nickel-bearing electroplating industrial effluents, J. Hazard. Mater.,s 119 (2005) 251–254.
[42] A. Faki, M. Turan, O. Ozdemir and A.Z. Turan, Analysis of fixed-bed column adsorption of Reactive Yellow 176 onto surfactant-modified zeolite, Ind. Eng. Chem. Res., 47 (2008) 6999–7004.